International Journal of Recent Technology and Engineering (IJRTE)
ISSN: 2277-3878, Volume-7, Issue-6S, March 2019

Finite element modeling and analysis of a de-bonded smart beam in actuation

Mohammad Mursaleen Butt, Sheikh Nazir Ahmad, Abdulrehman A. Al-Robaian, and Sher Afghan Khan

Abstract--- Stress, strain and displacement-based analysis of smart beam with debonding under actuation has been carried out. In this regard variational formulation based finite element modeling of a smart beam under actuation with debonding on the top and a bottom piezo layer has been developed. To know the proper functioning of the model, debonding at the center of the span and one-third of the span at the top and bottom interfaces between core and the piezo patches has been considered. Higher order beam bending for both host and piezo layers has been incorporated in the model. Due to debonding the number of degrees of freedom increase according to the number of elements considered along debonding portion. It can be observed that the results exhibit symmetry about centroidal axis which guarantees that the finite element model functions satisfactorily. Electric field along longitudinal and transverse directions does not change with regards to bonding and debonding in actuation. The pattern of axial displacement, normal strain and normal stress through thickness along span is found to be not affected by the debonding in actuation which is contrary to sensing. Which means the smart beam with debonding does not degenerate in actuation for axial displacement, normal stress and normal strain. The magnitudes of shear stress and shear strain at the root are minimum as compared to the magnitudes at the tip of the smart cantilever. However, the difference between bonding and debonding with regards to shear stress and shear strain is predominant at the root than at the tip. Which means the smart beam does not degenerate in debonding with regards to shear strain and shear stress.

Keywords: Smart Beam; Polarization; PZT-5H; Debonding

1. INTRODUCTION

Active structures have been designed, fabricated, analyzed and tested by various research organizations. These structures have found their applications in structural health monitoring, vibration and noise control, actuation and sensing etc. The analysis needs formulation of electro-thermo-elasticity-based development of governing equations. These equations can be derived by using the laws of conservation of mass, momentum, angular momentum, charge and energy [1-9]. The governing equations so developed can be used to develop variational formulation.

To analyze complex geometries like smart cantilever beams, finite element modeling based on variational formulation has been carried out. The evolution of this research field has matured enough to cover all the sub fields. Analysis of debonding in smart structures has been of interest to the researchers as this phenomenon degenerates the effectiveness of the structure.

The first thermo-elastic formulation was given by Coleman [10]. Micro deformations and rotations have been considered along with the laws of physics to formulate the thermo-elastic problem. Tiersten [11] has assumed the solid to be made up of material and electronic continuum which separate from each other under the application of external electric field. Laws of conservation of charge, mass, momentum, angular momentum and energy have been used to develop governing equations and boundary conditions. Ahmad et al. [12] has based his electro-thermo-elastic formulation on the pattern of Tiersten and has given the governing equations and boundary conditions in a use full form. The governing equations have been used to develop variational formulation for electro-thermo-elasticity. The interaction between electric field and polarization has been brought about. Ahmad et al. [13] has brought about difference between actuation and sensing by presenting induced potential, deflection, stress and strain in sensing and actuation respectively in a smart cantilever. Crawley and Luis [14] have designed and analyzed smart beam for actuation and sensing. It was found that discrete piezo patches effectively control the shape of a smart beam. The results have been correlated with known results. Zhang and Sun [15] have given analytical model for the analysis of smart beam in extensional and shear actuation beam. It has been shown that shear mode actuation is superior than extensional mode actuation. This is due to the reason that piezo material being brittle, therefore it cannot sustain normal stresses.

The recognition of importance of modeling and analysis of debonding in smart layered/composite structures has been that of a later stage. Tadashige et al. [16] have presented linear and nonlinear mathematical model for the analysis of a pair of partially debonded layers of a smart beam using Timoshenko beam theory. Bending and extension behavior for static conditions has been investigated. Strain distribution in the debonded region shows that the cracks in the actuator may occur before buckling in the extension mode.

Liyong Tong et al. [17] have presented the analytical method for sensing and actuation analysis of smart beam with debonding. Using classical beam theory, the analysis has been made based on axial and transverse beam theory. The stresses transferred through adhesive layer have been considered zero. It has been shown that debonding can have remarkable effects on internal forces, strains and frequency

Revised Manuscript Received on March 10, 2019.

Mohammad Mursaleen Butt, Mechanical Engineering Department, NIT Srinagar India-190006

Sheikh Nazir Ahmad, Mechanical Engineering Department, National Institute of Technology Kashmir, India

Abdulrehman A. Al-Robaian, Mechanical Engineering Department, Qassim University, Buraidah, Saudi Arabia

Sher Afghan Khan, Mechanical Engineering Department, Faculty of Engineering, International Islamic University, Kuala Lumpur, Malaysia (sakhan06@gmail.com)

spectrum. Axial force, shear force and bending moment along span are different for debonding as compared to fully bonded beam. End debonding has more effect on tip deflection than debonding at the middle of the span. Sun et al. [18] have analyzed the control stability of a debonded beam in actuation. From a bending extension model, characteristic equation of the beam controlled by partially debonded actuator and sensor layer has been derived. It has been found that even small edge debonding destabilizes the beam whereas in sensing the beam exhibits stability. Butt and Ahmad [19] have presented variational formulation for modeling the debonding in a smart cantilever. The beam has been analyzed in sensing mode under mechanical load. Since the cantilever is under a bending moment which varies from zero at the tip up to a maximum value at the root, the induced potential varies from least value at the tip to a maximum value at the root. The debonded beam has been shown degenerating under sensing of a mechanical load.

In most of the research works quoted above, electric potential has been assumed to be linear function of thickness coordinate. This decouples the bending induced voltage generated in the piezo patches. Moreover, classical beam bending elements or Timoshenko beam bending assumption has been incorporating in analyzing the smart beam. Whereas in the present study electric potential has been assumed to be quadratic function of thickness coordinate as:

$$\phi(x,z) = \phi_0 + z\phi_1 + cz^2\, d_2w/\, dx^2 \qquad (1)$$

This couples the bending and induced electric potential. The objectives of this study are:

1. Development of electro-thermo-elastic formulation for the analysis of actuation of a smart beam with symmetrically induced debonding between interfaces at the mid span. Based on this formulation variational formulation development results in finite element formulation.

2. Axial/transverse displacement, stress and strain computation of a symmetrically debonded smart beam in actuation.

2. MATHEMATICAL MODELING

Based on laws of physics i.e., conservation of momentum, angular momentum, charge, mass and energy, the governing equations have been developed. These governing equations are equilibrium equation, electrostatic equation and heat flux equation. Besides this there are constitute equations. The equilibrium equations have been integrated with respect to their variational variables to develop governing equations and boundary conditions. The governing equations have been used to develop finite element modeling for the analysis of debonding in smart beam in actuation mode. The four noded model finite element contains four axial degrees of freedom per node, three electric potential and one transverse displacement degrees of freedom per node. It makes a four noded element with eight degrees of freedom per node. This generates a stiffness matrix of the order of 32x32 for polarised medium and 20x20 order for non-polarised medium.

2.1. Electro-thermo-elastic equilibrium equations

The conservation of momentum at a point in polarized medium leads to summation of mechanical force, electrostatic force and gravitational force to be equated to inertial force. The equation can be written as:

$$\frac{\partial \sigma_{il}}{\partial x_l} + B_i + P_l E_{i,l} = \rho_m \frac{dv_i}{dt} \qquad (2)$$

Where σ_{lm} is stress tensors, **E** is the electric field vector, **P** is the polarization per unit volume, **B** is the gravity force per unit volume, v is the velocity vector and ρ is the density of the polarized medium. Stress tensor has two parts symmetric and anti-symmetric. The antisymmetric part is: $\sigma_{ij}^A = \frac{1}{2}(E_iP_j - P_iE_j)$

If polarization vector is in same direction as electric field vector, then antisymmetric stress tensor vanishes. In the present debonding analysis $\sigma_{ij}^A = 0$.

The conservation of charge results in electrostatic equation as; $D_{i,j} = 0$, where D is the electric displacement vector. Electric field and electric potential are related as. $\vec{E} = -\vec{\nabla}\phi$.

The thermal equilibrium equation for quasi-static deformation without heat generation is given as; $q_{i,i} = 0$, where q is the heat flux vector.

2.2. Constitutive equations

Equilibrium equations alone are not sufficient for finding all the unknown quantities at a point in a polarized medium i. e, six stresses, six strains, one temperature, three heat fluxes, one electric potential and one entropy. The conservation of energy results in following constitute equations;

$$\sigma_{i,j} = C_{ijmn}\,\varepsilon_{mn} - e_{i,jl}E_l - \alpha_{ij}\theta \qquad (3)$$

$$D_i = e_{ijmn}\,\varepsilon_{mn} - b_{j,n}E_n \qquad (4)$$

$$\varepsilon_0 E' + P' = D \qquad (5)$$

2.3. Variational formulation

The static variational formulation is obtained by integrating over volume the equilibrium equations multiplied by their respective variations as:

$$\iiint \left(\sigma_{il,j} + p_i E_{i,j}\right)\delta u_l dv + \iiint D_{m,m}\delta\phi\, dv = 0 \qquad (6)$$

Using Gauss divergence theorem

$$\iiint \sigma_{i,j}^L \delta\varepsilon_{i,j} dv - \iiint D_m \delta E_{i,j}\, dv = \iint T_i \delta u_i dA \qquad (7)$$

Where T_i represents the traction force per unit area of surface S.

3. BEAM MODEL

The debonded beam model shown in Fig.1 has been chosen for actuation analysis. The cantilever has aluminum core and PZT-5H full length piezo patches assumed to be brazed at the top and bottom of the aluminum core. The polarization axis in both the top and bottom patches is in the positive z-direction. The piezo material is transversely isotropic, and the aluminum core is isotropic. Higher order beam theory has been used for both core and piezo layers. The constitute equation for the piezo material is as:

Published By:
Blue Eyes Intelligence Engineering
& Sciences Publication

$$\{\mathrm{D_x}\ \mathrm{D_y}\ \mathrm{D_z}\ \sigma_x\ \sigma_y\ \sigma_z\ \sigma_{yz}\ \sigma_{xz}\ \sigma_{xy}\}^{\mathrm{T}} = \begin{Bmatrix} \epsilon_1^s & 0 & 0 & 0 & 0 & 0 & 0 & e_{15} & 0 \\ 0 & \epsilon_1^s & 0 & 0 & 0 & 0 & e_{15} & 0 & 0 \\ 0 & 0 & \epsilon_3^s & e_{31} & e_{31} & e_{33} & 0 & 0 & 0 \\ 0 & 0 & -e_{31} & c_{11}^E & c_{12}^E & c_{13}^E & 0 & 0 & 0 \\ 0 & 0 & -e_{31} & c_{12}^E & c_{11}^E & c_{13}^E & 0 & 0 & 0 \\ 0 & 0 & -e_{33} & c_{13}^E & c_{13}^E & c_{33}^E & 0 & 0 & 0 \\ 0 & -e_{15} & 0 & 0 & 0 & 0 & c_{44}^E & 0 & 0 \\ -e_{15} & 0 & 0 & 0 & 0 & 0 & 0 & c_{44}^E & 0 \\ 0 & 0 & 0 & 0 & 0 & 0 & 0 & 0 & c_{66}^E \end{Bmatrix} \begin{Bmatrix} E_x \\ E_y \\ E_z \\ \epsilon_x \\ \epsilon_y \\ \epsilon_z \\ \gamma_{yz} \\ \gamma_{zx} \\ \gamma_{xy} \end{Bmatrix} \quad (8)$$

Where ϵ_i^s *refers* to components of dielectric permittivity tensor. e_{ij} refers to piezoelectric constants and $c^E{}_{ij}$ refers to elastic constants. Each x–z layer of the beam has been assumed to be in the state of plane strain with normal stress in the z direction as zero.

3.1. Reduced constitutive relations

Each x–z layer being assumed in the state of plane strain with normal stress σz = 0 being zero, leads to; $\gamma yz = \gamma xz = \varepsilon y = 0$ and σz = 0 in each layer. This leads to following reductions in the constitutive equations;

$$\sigma_x = c^*\epsilon_x - e^*E_x \quad (9)$$

$$D_x = D_3 = \epsilon_3^s E_x + e_{31}\epsilon_x + e_{33}\epsilon_x \quad (10)$$

$$D_y = 0 \quad (11)$$

$$D_z = e_1^s E_z + e_{15}\gamma_{xz} \quad (12)$$

Where c*= (c_{33}-(c_{13}^2/c_{11}) for both piezo and metallic materials and

e*= (e_{33}- e_{31} $_{c13/c11}$) for piezo-material.

3.2. Finite element formulation

A four-node finite element beam bending element has been chosen for the analysis. Each node has four axial and one transverse degrees of freedom for both piezo and non-piezo materials. Exclusively for piezo material, three degrees of freedom per node for electric potential have been chosen. This makes a 32x32 order finite element model for the piezo material and 20x20 order stiffness matrix for the non-piezo material. Implementing the assumptions

$$\overline{u}_i^{l,I_j}(x) = \sum_{k=1}^{4} u_{ik}^{l,I_j}\, N_k\{\, \xi(x)\} \quad (13)$$

$$\overline{\phi}_i^{l,I_j}(x) = \sum_{k=1}^{4} \phi_{ik}^{l,I_j}\, N_k\{\, \xi(x)\} \quad (14)$$

And transverse displacement

$$w^{I_j}(x) = \sum_{k=1}^{4} u_k^{I_j}\, N_k\{\, \xi(x)\} \quad (15)$$

Where u_{ik}^{l,I_j}, ϕ_{ik}^{l,I_j} and $w^{I_j}(x)$ are the nodal degrees of freedom in I_j -th element in the l-th layer.

3.3 Validation of finite element model

For validation of the finite element model following dimensions of the aluminum cantilever, fully patched at the top and bottom surfaces with PZT-5H material have been given. The polarization axis in both the piezo patches has been assumed to be in positive z-direction. Beam length, L=100mm Aluminum Core thickness, t=16mmPiezo layer thickness, t=1mmApplied voltage at the top and bottom surfaces has been uniformly taken to be 10Volts. Width of the beam is unity. The interfaces between piezo patches and core material have been assumed to be grounded. The tip deflection found in actuation of 10Volts has been found to be 5.914×10^{-7}m. This value is near with the available results from literature. The convergence test has been carried out which has been found satisfactorily working beyond four elements along span.

4. RESULTS AND DISCUSSION

DE-BONDED BEAM MODEL

For the analysis of debonding in a smart cantilever in actuation mode, the interfaces between piezo patches at the top and bottom have been assumed to be debonded for a portion of one third of the span situated at the centre of the length of the beam. This type of model checks for the behaviour of the beam under actuation mode when the debonding has been placed at the top and bottom interfaces of the beam symmetrically.

4.1 Electric field in actuation

The top and bottom surfaces of the smart cantilever Fig. 1 have been actuated uniformly by 10 Volt and the interfaces between piezo patches and the core have been grounded. It means along x direction the electric field given by $E_{xx} = -(\partial\varphi)/(\partial x)$ has zero values at all entries as (10 Volt -10 Volt) difference is equal to zero. Therefore, there is no meaning of plotting electric field in x direction. In the z direction, the electric field given by $E_{zz} = -(\partial\varphi)/(\partial z)$ will be having same entries at every nodal point for bonding and debonding cases because everywhere (10Volt-5 Volt) difference is the same. So, there is no meaning of plotting the electric field in z direction. Overall the electric field values in x and z directions are same for both bonding and debonding cases. Hence debonding cannot have any effect in actuation with regards to electric field.

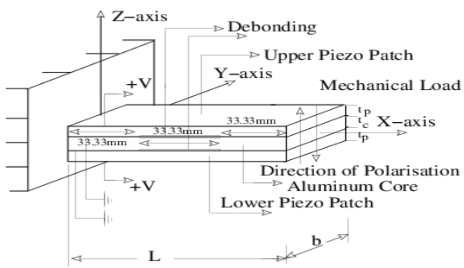

Fig. 1. De-bonded Smart Beam

4.2 Axial and transverse displacement field in actuation

The difference between transverse deflection between bonded and debonded beam is not pronounced. Same is the case with the axial displacement and Fig. 2. It means from the point of view of axial and transverse displacement, the debonded beam does not degenerate in actuation. The reason being that the top piezo full-length patch expands and bottom one shrinks without applying any shear force at any location of the beam to generate shear stress in the z-direction. It means the beam is under uniform pure bending moment from root to the tip. Therefore, no difference between bonding and debonding case is felt in transverse/axial displacements under actuation of 10Volts uniformly applied at the top and bottom piezo surfaces keeping interfaces between piezo and core surfaces grounded.

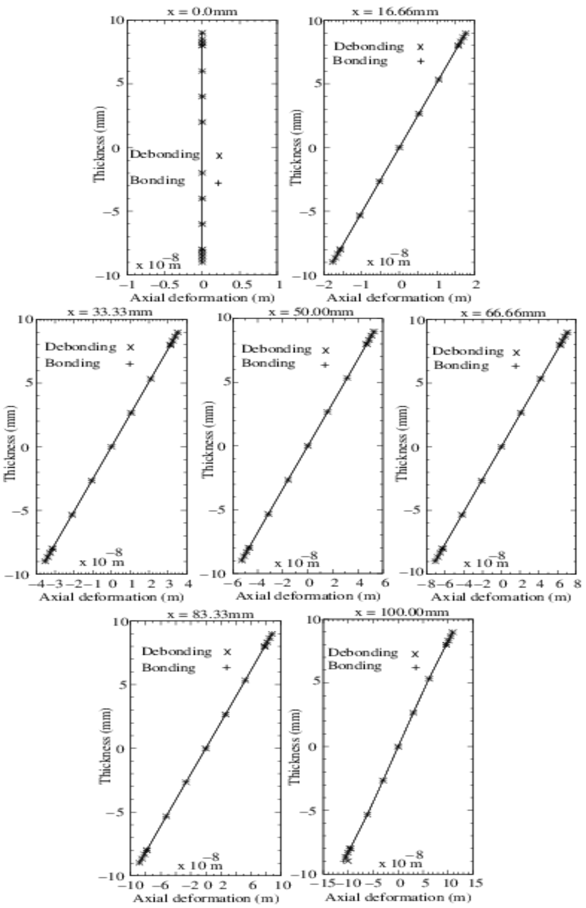

Fig. 2. Axial Deformation in De-bonded Beam in Actuation

4.3 Normal strain in actuation

Strain is purely dependent on displacements in axial and transverse directions. Since these displacements are similar between bonding and debonding in actuation therefore normal strain too remains unchanged. This can be noticed from Fig. 3

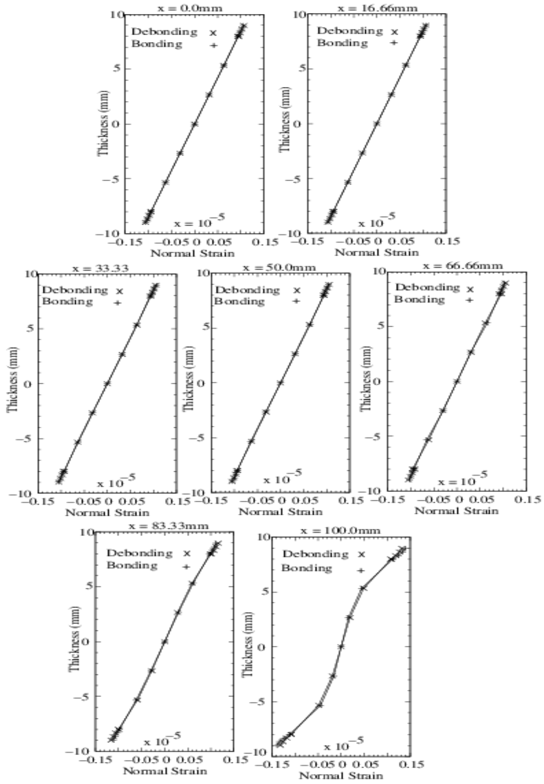

Fig. 3. Normal Strain in De-bonded Beam in Actuation

4.4 Normal stress in actuation

As observed from the Fig. 4, the normal stress in bonding case has major discontinuity at the interfaces due to material properties being different between piezo and core material. From constitutive equation, it can be observed that normal stress depends on normal strain multiplied by the material properties and added to the electric field (multiplied by the dielectric properties of piezo material in z-direction). However, there is no difference between normal strain between bonding and debonded case because strain depends on the difference between displacements divided by the elemental length. The finite element model used in this research ensures the continuity of strain at the interfaces which ensures the proper functioning of the finite element model. Since in actuation every longitudinal element is subjected to pure bending therefore the effect of debonding on normal stress does not show any variation.

Published By:
Blue Eyes Intelligence Engineering
& Sciences Publication

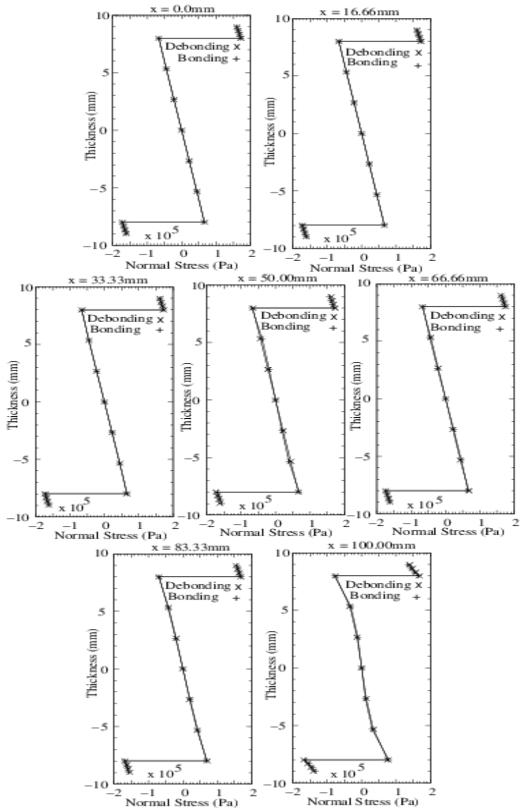

Fig. 4. Normal Stress in De-bonded Beam in Actuation

4.5. Shear strain in actuation

It can be noted from Fig.5 that with regards to shear strain the effect of deobnding is more towards root and at mid span of the beam than at the tip. The debonding effect is least at the tip about to the shear strain. At the interfaces for the portion of the debonding, the shear strain is zero where as it increases for same interface in bonded case.

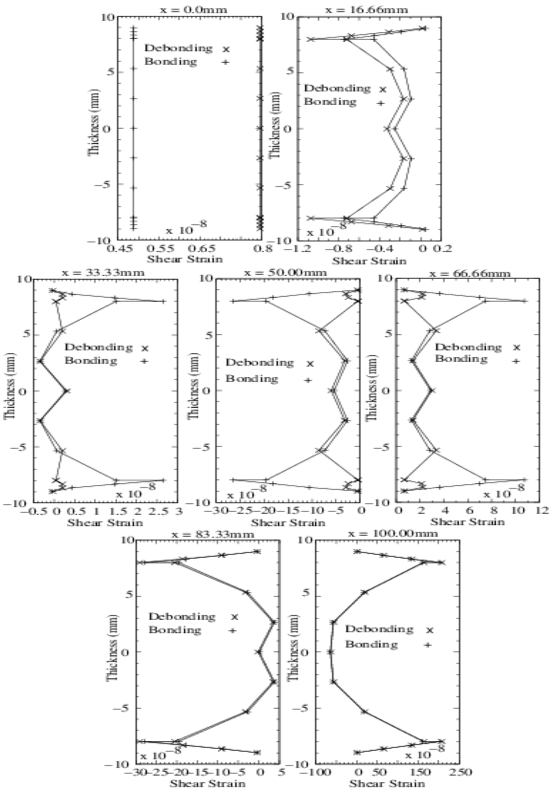

Fig. 5. Shear Strain in De-bonded Beam in Actuation

4.6 Shear stress along thickness in actuation

Fig. 6 shows the variation of shear stress through thickness from root to the tip at various locations on the span of the smart cantilever for both the bonded and debonded beam. It can be observed that the shear stress effect due to debonding is more predominant near root than it is at the tip. At the centre of the debonding portion along span, shear stress effect due to debonding is seen more than at the extremes of the debonding length. The magnitudes of shear stress at the root are negligible as compared to the magnitudes of shear stress at the tip. However, the difference between shear stresses with regards to bonding and debonding actuation at root is more as compared to that at tip of the smart beam. The reason for this is that shear strain increases from root to the tip in sensing.

4.7 Shear stress along span in actuation

Referring to the Fig. 7 it can be noticed that the magnitude of shear stress at the interfaces between piezo and core layers increases in the positive sense from two third of span onwards. The shear stress along span at the middle of the core increases in the negative sense from two third of span onwards. This behaviour is seen despite the fact whether the case is fully bonding or debonding. Since a mechanical shear force is missing in actuation from root to the tip therefore the magnitude of shear stress is negligible up to two third of the span at interfaces as well as at the mid layer. From two third onwards of the span the shear stress grows at the interfaces as well as at the mid layer only due to the reason that the magnitude of the shear strain increases at higher rate toward tip of the beam in actuation.

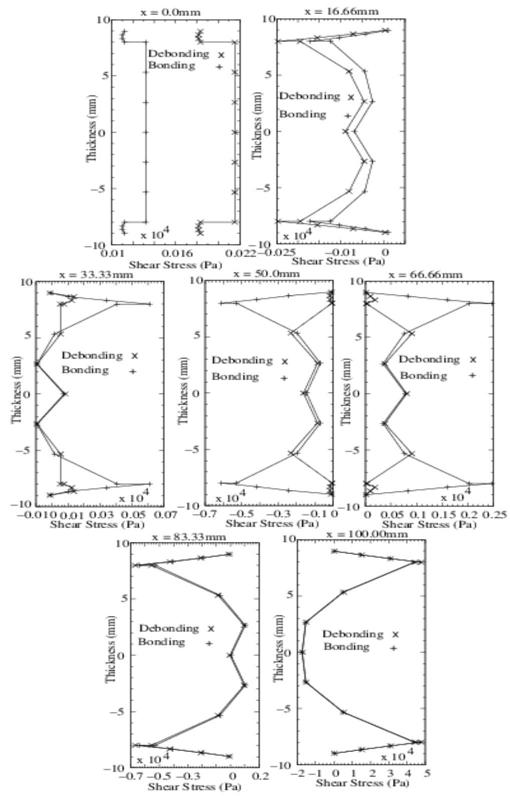

Fig. 6. Shear Stress in De-bonded Beam in Actuation

Published By:
Blue Eyes Intelligence Engineering
& Sciences Publication

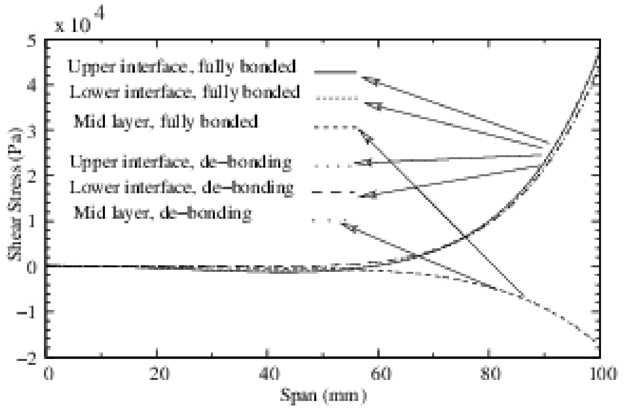

Fig. 7. Shear Stress along Span in De-bonded Beam in Actuation

5. CONCLUSION

The analysis of a smart cantilever beam in actuation mode with debonding at the top and bottom interfaces between piezo and core materials symmetrically located at the centre and one third portion of the span has been carried out. The variation in axial displacement/strain/stress and shear-strain/stress through thickness and along span for bonding and debonding of smart cantilever has been presented under electric actuation. The following are the conclusions of the analysis;

1. Since the smart beam is under actuation of 10Volts uniformly at the top and bottom free surfaces while interfaces between piezo layers and core of the beam have been grounded, there is no difference between axial and transverse electric field in the bonding and debonding cases for electric actuation.
2. Since the smart beam under 10Volt actuation comes under constant bending moment from root to the tip therefore here is no difference between axial displacement, normal strain and normal stress for bonding and debonding cases. Hence the smart beam with debonding does not degenerate with regards to axial displacement, normal strain and normal stress under electric actuation.
3. Magnitude of shear stress and shear strain is lowest at the root and maximum at the tip of the smart cantilever. However, the difference between shear strain and shear stress is more at the root and less at the tip between the bonding and debonding cases under electric actuation. This means the smart cantilever does not degenerate in debonding with regards to Shear strain and shear stress in actuation. This is contrary to a smart beam with debonding in sensing with mechanical load.

REFERENCES

1. Cady, W. G., (1964), "*Piezoelectricity an Introduction to the Theory and Applications of Electro-mechanical Phenomena in Crystals*," Vol. 1, Dover, New York.
2. Ikeda,T., (1990), "*Fundamentals of Piezoelectricity*", Oxford Univ. Press, Oxford.
3. Nalwa, H. S, (1999), "*Handbook of Low and High Dielectric Constant Materials and Their Applications*", Vol. 2: Phenomena, Properties and Applications, Edited, Academic Press.
4. Landau, L. D., Lifshitz, E. M., and Pitaevski, L. P., (1984) "*Electrodynamics of Continuous Media"*, 2nd ed., Vol. 8, Pergamon, New York.
5. Hellen, E., (1962), "*Electromagnetic Theory"*, 1st ed. John Wiley & Sons Inc., New York.
6. Griffiths, D. J., (1999), "*Introduction to Electrodynamics*", 3rd ed., Prentice-Hall, India, 1999.
7. Tiersten, H. F., (1969) "*Linear Piezoelctric Plate Vibrations, Elements of the Linear Theory of Piezoelectricity and the Vibrations of Piezoelectric Plates*", 1st ed., Plenum Press, New York.
8. Gurtin, M. E., (1981), "*Mathematics in Science and Engineering, An Introduction to Continuum Mechanics"*, 1st ed. Vol. 158, Academic Press, New York.
9. Malvern, L. E., (1969) "*Introduction to the Mechanics of a Continuous Medium"*, 1st ed., Prentice-Hall, Inc. New Jersey.
10. Landau, L. D., and Lifshitz, E. M., (1970), "*Theory of Elasticity"*, 2nd ed., Vol. 7, Pergamon, New York.
11. Coleman, B. D., (1964) "Thermodynamics of Materials with Memory," *Journal of Rational Mechanical Analysis*, Vol. 17, No. 1, pp. 1-46.
12. Tiersten, H. F., (1971), "On the Nonlinear Equations of Electro-thermo-elasticity," *International Journal of Engineering Sciences*, Vol. 9, No. 7, pp. 587-604.
13. Ahmad, S. N., Upadhyay C. S., and Venkatesan C., (2006), "Electro-thermo-elastic Formulation for the Analysis of Smart Structures," *Journal of Smart Materials and Structures*, No. 15, pp. 401-416.
14. Ahmad, S. N., Upadhyay C. S., and Venkatesan C., (2004), "Linear and Non-linear Analysis of a Smart Beam Using General Electro-thermo-elastic Formulation", *AIAA Journal*, 42(4), pp. 840-849.
15. Crawley, E. F., (1994), "Intelligent Structures for Aerospace: A Technological Overview and Assessment," *AIAA Journal*, Vol. 31, No. 8, pp. 1689–1699.
16. Zhang, X. D., and Sun, C. T., (1996), "Formulation of an Adaptive Sandwich Beam," *Smart Materials and Structures*, Vol. 5, No. 6, pp. 814–823.
17. Tadashige, I., Samikkannu R., and Tetsuhiko, U., (2010), "Deformation of a Beam with Partially De-bonded Piezoelectric Actuators," *Journal of Intelligent Materials Systems and Structures*, Vol. 21. No. 3.
18. Liyong, T., Dongchang, S., and Satya, N. A., (2001), "Sensing and Actuating Behaviours of Piezoelectric Layers with Debonding in Smart Beams," *Smart Mater. Struct*. Vol. 10. pp. 713–723.
19. Dongchang, S., and Liyong, T., (2002), "Control Stability Analysis of Smart Beams with De-bonded Piezoelectric Actuator Layer," *AIAA Journal* Vol. 40, No. 9, pp. 1852-1859.
20. Butt, M. M., and Ahmad. S. N., (2017), "Modeling and Analysis of Debonding in a Smart Beam in Sensing Mode Using Variational Formulation," *Journal of King Saud University-Science*, pp. 1-15.
21. https:\\doi.org\10.1016\j.jksus.2017.08.013, 2017

Published By:
Blue Eyes Intelligence Engineering
& Sciences Publication